PAPER • OPEN ACCESS

Fast 3D simulation of various applications of induction heating

View the article online for updates and enhancements.

Fast 3D simulation of various applications of induction heating

H.K. Bui, A. Ba, G. Berthiau, D. Trichet

Laboratory IREENA
University of Nantes, France

Corresponding author: Gerard.Berthiau@univ-nantes.fr

Abstract
In this paper, we present some advances in 3D finite element modeling of the induction heating process. Lighten finite element models are used for fast simulation of Carbone Fiber Reinforced Polymers and massive metals at high frequencies. The lightening methods include the use of degenerated hexahedral Whitney elements for very thin anisotropic layers and the impedance boundary condition with external electrical circuit constraint.

Keywords: 3D FEM, Degenerated Whitney Elements, Impedance Boundary Condition, Induction Thermography NDT, Induction Heating.

Introduction
In this work, various applications of induction heating including welding and nondestructive testing (NDT) are presented. For metal material and carbon fiber reinforced polymers (CFRP), induction welding has already proved its efficiency whereas induction thermography may provide a very promising NDT method [1]. In induction thermography, the presence of defect leads to abnormal temperature distribution on the surface of the piece which can be revealed on the thermal image measured by an infrared thermal camera [2].

Simulation software using finite element method (FEM) provides a powerful tool for the design and optimization of the techniques [3]. However, simulations at high frequencies with external circuit coupling using classical FEM are very time consuming. For CFRP, classical FEM must deal with the numerical issues of very thin and anisotropic multi-layers region which also leads to high computation time.

In this work, we present fast and accurate 3D finite element models for coupled electromagnetic thermal simulation of induction heating processes. For CFRP, the electromagnetic model is lightened by using degenerated hexahedral Whitney elements. For strong skin effect simulations, the electromagnetic model is lightened by means of the Surface Impedance Boundary Condition (SIBC) [4] applied to both the massive induction coil surface taking into account the coupled external electrical circuit and the surface of the conductor work-piece. In this case, the thermal diffusion in the work-piece is solved using surface electromagnetic power density as thermal source. Applications on induction welding and induction thermography NDT are shown.

Classical mathematical formulation
The weak electromagnetic $\boldsymbol{A} - \psi$ and thermal formulations (1) and (2) can be used to calculate induced electromagnetic fields and temperature distribution in the conductor body:

$$\int_{\Omega} \left(\boldsymbol{curlN_e} \frac{1}{[\boldsymbol{\mu}]} \boldsymbol{curlA} + [\boldsymbol{\sigma}](\boldsymbol{N_e} + \boldsymbol{gradN_n}) \, j\omega(\boldsymbol{A} + \boldsymbol{grad\psi}) \right) d\Omega - \int_{\Gamma} \boldsymbol{N_e} \left(\boldsymbol{n} \wedge \frac{1}{[\boldsymbol{\mu}]} \boldsymbol{curlA} \right) = \int_{\Omega} \boldsymbol{N_e} \boldsymbol{J_s} d\Omega \qquad (1)$$

$$\int_{\Omega_c} \left(\rho C_p \frac{\partial T}{\partial t} - div[\boldsymbol{\lambda}] \boldsymbol{gradT} \right) N_n \, d\Omega = \int_{\Omega_c} P N_n \, d\Omega \qquad (2)$$

where $\boldsymbol{A}$ and ψ are respectively the magnetic vector potential and the primitive in time of electric scalar potential, J_s the source current density, P the electromagnetic induced power density, T the temperature, C_p the specific heat, ρ the specific mass of the material, $[\boldsymbol{\sigma}]$ and $[\boldsymbol{\lambda}]$ respectively the tensors of electrical and thermal conductivity which are function of fiber orientation θ^i. The edge shape function and nodal shape function are denoted by $\boldsymbol{N}_e$ and N_n respectively.

Degenerated hexahedral Whitney elements

The degenerated nodal elements are determined by:

$$(N_n^2 \qquad , N_n^2 \qquad) \tag{3}$$

where N_n^{2D} denotes the nodal elements defined on the quadrilateral mesh of the upper and lower surfaces of the thin region which are:

$$
\begin{aligned}
&= (1-u)(1-v)/4, \quad = (1+u)(1-v)/ \\
&= (1+u)(1+v)/4, \quad = (1-u)(1+v)/
\end{aligned} \tag{4}
$$

and $\quad = (1 \pm w)/2$ are the interpolation functions along the thickness of the region. The degenerated edge elements are written as:

$$(\boldsymbol{N}_e^2 \qquad , \boldsymbol{N}_e^2 \qquad , N_n^{2D}\boldsymbol{n}/\varepsilon) \tag{5}$$

N_e^{2D} is the set of edge elements defined on a quadrilateral, $\boldsymbol{n}$ the normal vector of median surface of the element, ε its thickness. In the case of a multi-layer region, double layer quadrilateral meshes are created to represent each layer of the region. The coefficients associated with the common edges and common nodes between two double layer meshes are the contribution of those calculated in each mesh. The left-hand side of the $\boldsymbol{A} - \psi$ formulation in the CFRP laminate domain Ω_c can be determined by [5]:

$$
\begin{aligned}
\int_{\Omega_c} \left(\boldsymbol{curlN}_e \frac{1}{[\boldsymbol{\mu}]} \boldsymbol{curlA} \right) d\Omega &= \sum_{i=1,k} \left(\int_S \frac{1}{\mu_{z,i}\varepsilon_i} [\boldsymbol{n} \wedge \boldsymbol{N}_e^{2D}][\boldsymbol{n} \wedge \boldsymbol{A}] \, dS \right) \\
&+ \sum_{i=1,k} \left(\int_S \frac{i}{[\boldsymbol{\mu}]_{xy,i}} \left(\int \langle \boldsymbol{rotN}_e^{2D} \rangle \langle \boldsymbol{rotA} \rangle dw \right) dS \right)
\end{aligned} \tag{6}
$$

$$
\begin{aligned}
\int_{\Omega_c} \left([\boldsymbol{\sigma}](\boldsymbol{N}_e + \boldsymbol{gradN}_n) \, j\omega(\boldsymbol{A} + \boldsymbol{grad}\psi) \right) d\Omega &= \sum_{i=1,k} \left(\int_S \frac{\sigma_{z,i}}{i} (\varepsilon_i \boldsymbol{n} \boldsymbol{N}_e + [N_n^{2D}])(\varepsilon_i \boldsymbol{n} \boldsymbol{A} + [\psi]) \, dS \right) \\
&+ \sum_{i=1,k} \left(\int_S [\boldsymbol{\sigma}]_{xy,i}\varepsilon_i \left(\int \langle \boldsymbol{N}_e^{2D} + \boldsymbol{gradN}_n^{2D} \rangle \langle \boldsymbol{A} + \boldsymbol{grad}\psi \rangle dw \right) dS \right)
\end{aligned} \tag{7}
$$

where k is the number of degenerated elements, $_i$ the thickness of element i, S the median surface of the CFRP laminate, $\mu_{z,i}$ and $\sigma_{z,i}$ the permeability and the electrical conductivity in the normal direction to the median surface of the material, $[\boldsymbol{\mu}]_{xy,i}$ and $[\boldsymbol{\sigma}]_{xy,i}$ the physical tensors of the material defined in the plan of its median surface. The symbols $\langle a \rangle = a \quad + a \quad$ and $[a] = a \quad - a$ denote respectively the weighted average of a function a over the thickness of the layer and the jump of a across the layer.

Case study 1

An induction welding case study is shown in this section. The piece to be heated is a 16 plies composite plate with the lay-up sequence $[135°/90°/45°/0°/135°/90°/45°/0°]_S$. The thickness of a ply is 140μm. An U-shaped coil is used in this study. It is placed right above the piece and centered on it. The excitation current intensity is of 200A RMS at 2MHz. The geometry of the composite plate and the inductor are shown in the Fig. 1. In the same figure, the simulated distribution of eddy current inside the plate is shown. The temperature rise after 5s of heating is shown in the Fig. 2. The induced power distribution depends strongly on the lay-up sequence of the composite. The temperature distribution can be controlled by means of inductor design and operational parameters choice.

Surface impedance boundary condition with external electrical circuit constraint

In this method, only the surface meshes of the conductors are required. The magnetic vector potential $\boldsymbol{A}$ is defined everywhere whereas electric scalar potential ψ is defined only on the surface of the conductors (inductor and pipe). On the surface of the conductors, one applies the SIBC:

$$\boldsymbol{n} \wedge \frac{1}{\mu} \boldsymbol{rotA} = \frac{1}{Z_c} \boldsymbol{n} \wedge \left(\boldsymbol{n} \wedge j\omega(\boldsymbol{A} + \boldsymbol{grad}\psi) \right) \tag{8}$$

where $\boldsymbol{n}$ is the outward normal vector of the surfaces of the conductors, Z_c the surface impedance which depends on the conductivity of the conductor. The $\boldsymbol{A} - \psi$ weak formulation with a voltage V imposed as external circuit condition [6][7] reads:

$$\int_{\Omega} \boldsymbol{curlN}_e \frac{1}{\mu} \boldsymbol{curlA}\, d\Omega + \int_{S} \frac{1}{Z_c} \big(\boldsymbol{n} \wedge j\omega(\boldsymbol{A} + \boldsymbol{grad}\psi)\big)(\boldsymbol{N}_{eS} \wedge \boldsymbol{n})dS = -\int_{S} \frac{1}{Z_c}(\boldsymbol{n} \wedge \boldsymbol{grad}V\alpha)(\boldsymbol{N}_{eS} \wedge \boldsymbol{n})dS \tag{9}$$

$$\int_{S} \frac{1}{Z_c}\big(\boldsymbol{n} \wedge j\omega(\boldsymbol{A} + \boldsymbol{grad}\psi)\big)(\boldsymbol{grad}N_{ns} \wedge \boldsymbol{n})dS = -\int_{S} \frac{1}{Z_c}(\boldsymbol{n} \wedge \boldsymbol{grad}V\alpha)(\boldsymbol{grad}N_{ns} \wedge \boldsymbol{n})dS \tag{10}$$

where $\alpha = \sum_{C_S} N_{nS}$ is the sum of all the nodal shape function defined on the contour of the electrodes (C_S) where the voltage V is imposed. S is the surface of the conductors (inductor and pipe). The case study 2 is presented as an application of this method to the NDT by induction thermography.
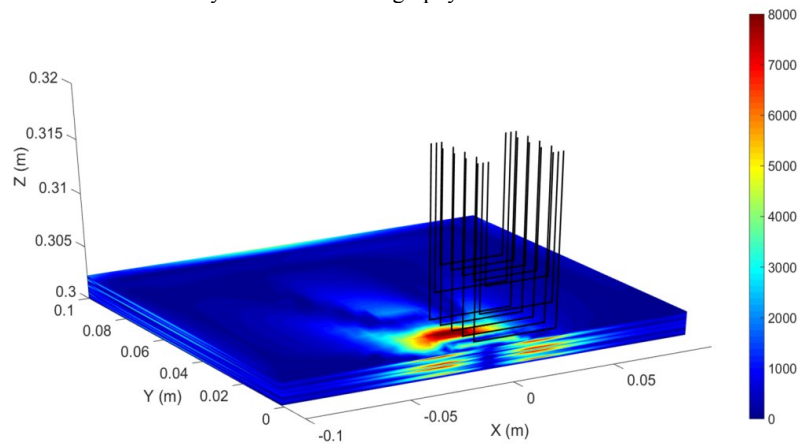

Fig. 1. Case study 1: Geometry of the composite plate and the U-shaped inductor. ½ of the plate ($x > 0$, $y > 0$) is shown.
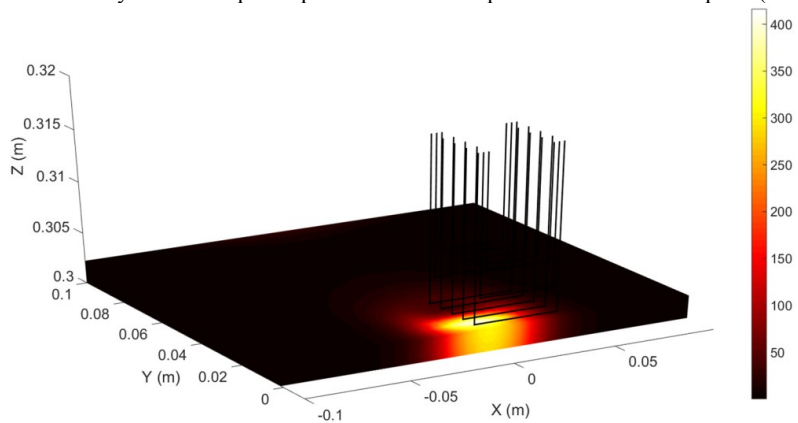

Fig. 2. Case study 1: Eddy current distribution in the plate. ½ of the plate ($x > 0$, $y > 0$) is shown.

Case study 2

An induction thermography study case is shown in this section. The piece to be inspected is a metal pipe with a vertical crack. A massive inductor is used to carry a high intensity current. The electrical conductivities of the pipe and the inductor are 2×10^6 S/m and 10^7 S/m respectively. The excitation electromagnetic frequency is 5kHz. The surface impedance boundary conditions are applied to both the surface of the pipe and the inductor.

The Fig. 3 shows the current density distribution in the inductor and eddy current in the pipe. The presence of the crack disturbs the circulation of eddy current and leads to a high current density around the crack tips due to the edge effect. This effect is highly observed on the temperature distribution after the heating as shown in the Fig. 4. In the practice,

this image can be observed and recorded using an infrared thermal camera. The crack defect can be then detected by this principal.
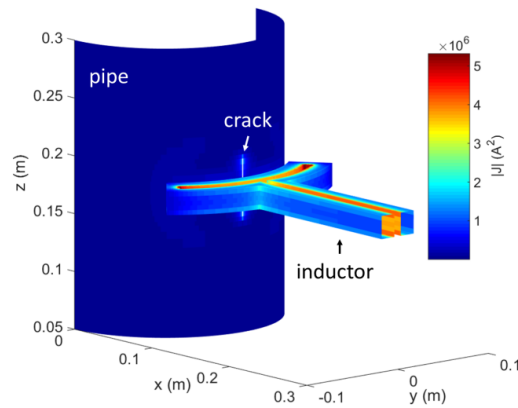

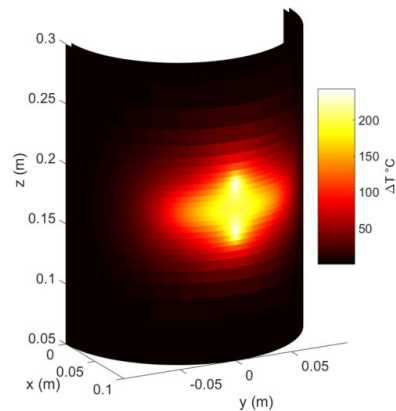Fig. 3. Case study 2: Current density distribution in the inductor and in the pipe with a crack defect.

Fig. 4. Case study 2: Temperature distribution showing the crack tips with higher temperature.

Conclusion

Degenerated hexahedral elements can be used to deal with thin and anisotropic layered materials such as carbon fiber reinforced polymers. The use of these elements can achieve the same accuracy as classical methods with reduced computation time. The surface impedance boundary condition can be implemented with external electrical circuit condition and provides a fast method to deal with simulation with strong skin effect.

Acknowledgment

References

1. J. Fouladgar (Edt.) (2012), Electrothermics, Wiley.
2. H.K. Bui, G. Wasselynck, D. Trichet, and G. Berthiau (2013), IEEE Trans. Magn., vol. 49, no. 5, 1949-1952.
3. H.K. Bui, G. Berthiau, D. Trichet and G. Wasselynck (2015), 8th Int. Conference on Electromagnetic Processing of Materials, Cannes (France), 403-406.
4. S. Yuferev, N. Ida (1999), IEEE Trans. Magn., vol. 35, no. 3,1486 - 1489.
5. H. K. Bui, G. Wasselynck, D. Trichet and G. Berthiau (2016), IEEE Trans. on Magn., vol. 52, no. 3.
6. S. M. Mimoune, J. Fouladgar, A. Chentouf, and G. Develey (1996), IEEE Trans. on Magn., vol. 32, no. 3, 1605.
7. A. Desmoort, Z. D. Greve, P. Dular, C. Geuzaine, and O. Deblecker (2017), IEEE Trans. on Magn., vol. 53, no. 6.